Cancer Letters 451 (2019) 34–47

Contents lists available at ScienceDirect

Cancer Letters

journal homepage: www.elsevier.com/locate/canlet

Original Articles

Blocking autophagy flux promotes interferon-alpha-mediated apoptosis in head and neck squamous cell carcinoma

Wenyi Yang[a,b,1], Chunlan Jiang[b,c,1], Weiya Xia[d], Houyu Ju[a,b], Shufang Jin[a,b], Shuli Liu[a,b], Liming Zhang[a,b], Guoxin Ren[a,b], Hailong Ma[a,b,***], Min Ruan[a,b,**], Jingzhou Hu[a,b,*]

[a] Department of Oral Maxillofacial-Head and Neck Oncology, Shanghai Ninth People's Hospital, College of Stomatology, Shanghai Jiao Tong University School of Medicine, Shanghai, 200011, China
[b] Shanghai Key Laboratory of Stomatology, Shanghai Research Institute of Stomatology, National Clinical Research Center for Oral Diseases, Shanghai, 200011, China
[c] Department of Prosthodontics, Shanghai Ninth People's Hospital, College of Stomatology, Shanghai Jiao Tong University School of Medicine, Shanghai, 200011, China
[d] Department of Molecular and Cellular Oncology, The University of Texas MD Anderson Cancer Center, Houston, TX, 77030, USA

ARTICLE INFO

Keywords:
Head and neck squamous cell carcinoma
Interferon-alpha
Hydroxychloroquine
Wortmannin
Autophagy

ABSTRACT

Despite multiple antitumor activities, interferon-alpha (IFNα) therapy alone is less effective in solid tumors. Autophagy has been reported to play a key role in tumor chemoresistance. Therefore, it is meaningful to explore whether autophagy can be activated by IFNα in head and neck squamous cell carcinoma (HNSCC) and serve as a potential target to improve efficacy of IFNα therapy. In this study, we report that IFNα not only exhibits anti-proliferation activity and induces apoptosis, but also activates autophagy in HNSCC cells. Moreover, silencing autophagy-related protein 5 (ATG5) and signal transducer and activator of transcription 1 (STAT1) suppresses autophagy flux. Furthermore, IFNα and autophagy inhibitors (hydroxychloroquine and wortmannin) show clear synergistic effects on inhibiting growth and promoting apoptosis in HNSCC cells and xenograft models. Our findings indicate that IFNα-induced autophagy plays a cytoprotective role and blocking autophagy flux promotes IFNα-mediated apoptosis in HNSCC. These results suggest that the combination of IFNα and autophagy inhibitors represents a novel strategy for HNSCC treatment.

1. Introduction

Head and neck squamous cell carcinoma (HNSCC) is one of the most frequent cancers with significant morbidity and mortality worldwide [1]. Despite comprehensive treatment methods including surgery, chemoradiotherapy and molecular targeting therapy, the 5-year survival rate is only approximately 65%. For patients with recurrence and metastasis, although cytotoxic chemotherapy is used, the median survival after palliative chemotherapy is approximately 4–10 months [2]. Therefore, it is necessary to develop new HNSCC treatment strategies.

Autophagy is a highly evolutionarily conservative cellular metabolic pathway. Accumulating evidences suggest that autophagy is a switchable mechanism in cancer progression [3,4]. Autophagy can inhibit the initial stages of carcinogenesis [5], but also support the survival and growth of established cancers [6–8]. Effective inhibition of autophagy in advanced cancers may contribute to treatment of malignancies. Several studies suggest that activation of the autophagy in HNSCC can either protect cells [9,10] or initiate type II programmed cell death [11,12]. Therefore, the roles and mechanisms of autophagy activated by specific drugs in HNSCC require further investigations.

Trials of interferon-alpha (IFNα) have yielded varied success in several tumors, such as malignant melanoma, Kaposi's sarcoma, and renal cell carcinoma [13]. Recent findings suggest that IFNα improves the efficacy of antitumor treatment for HNSCC based on various activities, including augmenting various immune functions [14], inhibiting tumor cell proliferation [15], and impeding tumor metastasis

* Corresponding author. Department of Oral Maxillofacial-Head and Neck Oncology, Shanghai Ninth People's Hospital, Shanghai Jiao Tong University School of Medicine, No 639, Zhizaoju Rd, Shanghai, 200011, China.
** Corresponding author. Department of Oral Maxillofacial-Head and Neck Oncology, Shanghai Ninth People's Hospital, College of Stomatology, Shanghai Jiao Tong University School of Medicine, Shanghai, 200011, China.
*** Corresponding author. Department of Oral Maxillofacial-Head and Neck Oncology, Shanghai Ninth People's Hospital, College of Stomatology, Shanghai Jiao Tong University School of Medicine, Shanghai, 200011, China.
E-mail addresses: mahl21@sjtu.edu.cn (H. Ma), ruanm1740@sh9hospital.org (M. Ruan), huyayi@shsmu.edu.cn (J. Hu).
[1] Wenyi Yang and Chunlan Jiang equally contributed to this work.

https://doi.org/10.1016/j.canlet.2019.02.052
Received 26 October 2018; Received in revised form 19 February 2019; Accepted 28 February 2019

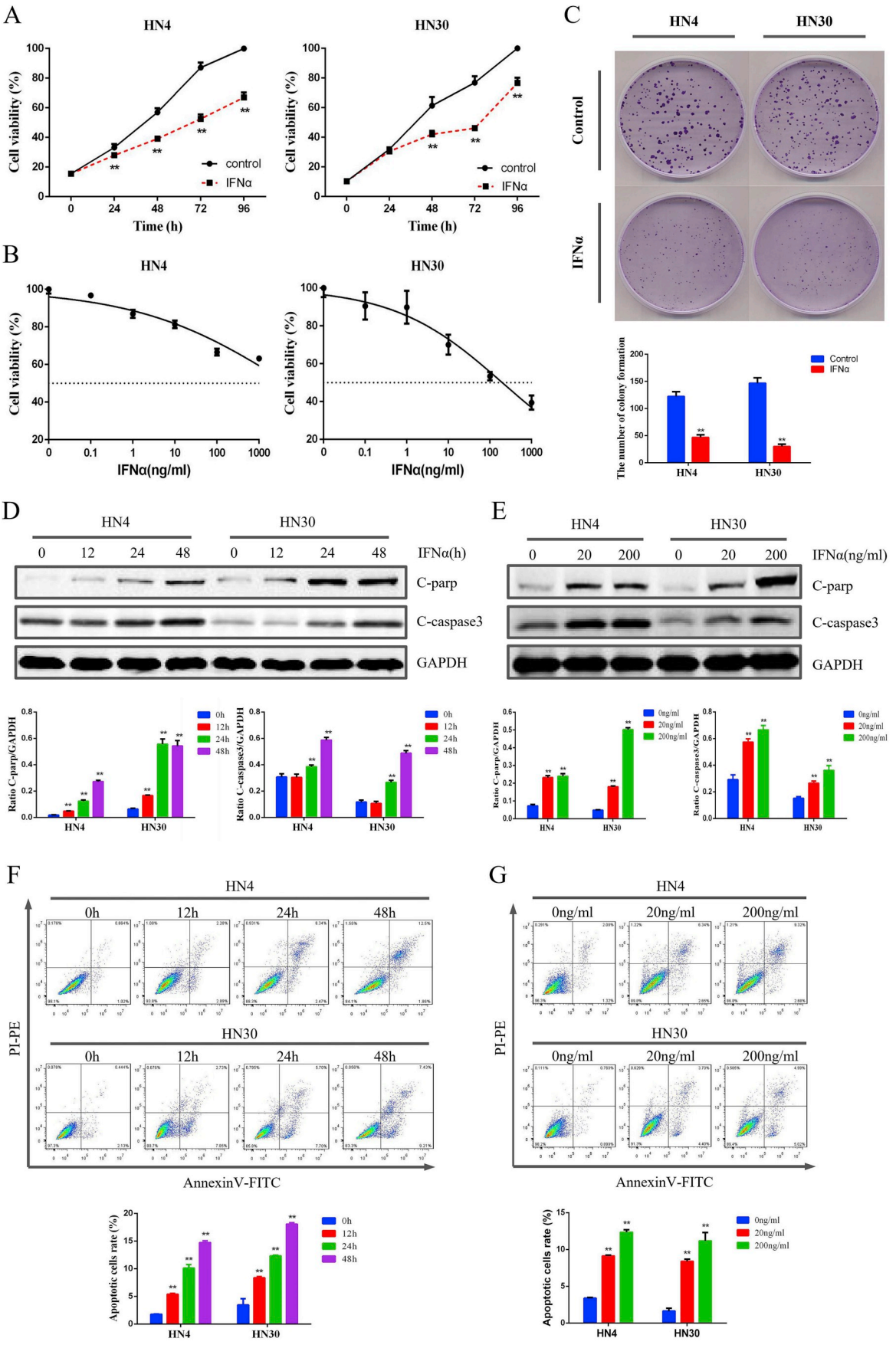

(caption on next page)

Fig. 1. IFNα exhibits anti-proliferation activity and induces apoptosis in HN4 and HN30 cells. (A) HN4 and HN30 cells were incubated with 20 ng/ml of IFNα or PBS for multiple time points, and then cell viability was measured using the MTT assay. (B) After treatment with the indicated concentrations of IFNα for 72 h, cell viability was measured using the MTT assay. (C) IFNα inhibited colony formation in HN4 and HN30 cells. Following treatment with IFNα (200 ng/ml) for 24 h, cells were incubated in new fresh complete medium for 10 days and stained with 0.5% crystal violet. Representative images of colonies were presented, and the bar graph represented the relative colony formation efficiencies. (D) Western blot revealed that PARP and caspase3 were activated after treatment with indicated concentrations of IFNα for indicated time points in HN4 and HN30 cells. Membranes were probed with a GAPDH antibody as a loading control. ImageJ densitometric analysis of the cleaved-PARP/GAPDH ratio and cleaved-caspase3/GAPDH ratio was shown. (E) Western blot showed PARP cleavage and activation of caspase3 after IFNα treatment (200 ng/ml) for 48 h in HN4 and HN30 cell lines. (F) After 200 ng/ml of IFNα treatment for indicated time points, apoptotic cell rates were analyzed by flow cytometry. (G) HN4 and HN30 cells were treated with indicated concentrations of IFNα for 24 h before staining with Annexin V and propidium iodide (PI), and the apoptotic rates were determined by flow cytometry. $^{**}P < 0.01$. (For interpretation of the references to color in this figure legend, the reader is referred to the Web version of this article.)

[16]. Our previous study [17] also demonstrates that IFNα can enhance the antitumor effects of erlotinib and nimotuzumab in HNSCC. However, IFNα has not been approved for most solid tumors, and IFNα therapy alone is less effective once the tumor has established [18,19], which is likely reflective of adaptive resistance and changes in IFNα signaling outcomes. Studies of chemoresistance in brain, gastric and ovarian cancers suggest that autophagy plays a key role in tumor chemoresistance [20–22]. Thus, it is meaningful to explore whether autophagy can be activated by IFNα in HNSCC and serve as a potential target in conjunction with IFNα therapy.

In our current study, we first demonstrate that IFNα induces autophagy in HNSCC cells. Moreover, STAT1 and ATG5 molecules are required for autophagy activated by IFNα. Furthermore, IFNα and autophagy inhibitors exhibit clear synergistic effects on inhibiting growth and promoting apoptosis *in vitro* and *in vivo*. This finding could contribute to the application of autophagy inhibitors for the improvement of IFNα therapy for HNSCC in the clinic.

2. Materials and methods

2.1. Cell culture

The cell lines used in this study included HN4, HN30, SCC25 and Cal27. The tongue squamous cell carcinoma cell lines SCC25 and Cal27 were purchased from ATCC (Manassas, VA, USA). The cell line HN4 was established from tongue squamous cell carcinoma, whereas HN30 was established from pharyngeal squamous cell carcinoma. HN4 and HN30 cell lines were kindly provided by the University of Maryland Dental School, USA. These cell lines were cultured in Dulbecco's modified Eagle's medium (DMEM) (Gibco, Carlsbad, CA) supplemented with 10% fetal bovine serum, 1% glutamine, and 1% penicillin-streptomycin. Cells were cultured in a humidified atmosphere containing 5% CO_2 at 37 °C.

2.2. Cell proliferation assay

HNSCC cells were plated in 96-well flat bottom plates at a density of 3×10^4 cells/ml. IFNα was administered at the indicated concentrations after cell adherence. The cell proliferation assay was performed using a 3 - (4, 5 – Dimethylthiazol – 2 - yl) - 2, 5 - diphenyltetrazolium bromide (MTT) solution (0.5 mg/ml). The plates were incubated in a humidified incubator at 37 °C for 4 h. Then, the medium was removed and formazan dye was solubilized with DMSO. The optical density (OD) was measured at an absorbance wavelength of 490 nm within 10 min.

2.3. Colony formation assay

To determine colony formation, HN4 and HN30 cells at the exponential growth phase were harvested, seeded at approximately 5×10^2 cells per cell culture dish and cultured in complete medium for 24 h. Cells were exposed to IFNα for 24 h. Then the cells were cultured in new complete medium for 10 days and finally rinsed with PBS twice, fixed with 100% methanol for 30 min and stained with 0.5% crystal violet for 20 min. The number of colonies formed was quantified using ImageJ software.

2.4. Real-time PCR assay

Real-time PCR assay was performed as previously described [23], following the manufacturers' instructions (Takara, Dalian, China). The primer sequences were as follows: GAPDH forward: 5' - CCTCTGACT TCAACAGCGAC - 3′ and reverse: 5' - TCCTCTTGTGCTCTTGCTGGC - 3'; P62 forward: 5' - CCGTGAAGGCCTACCTTCTG - 3′ and reverse: 5' - TCCTCGTCACTGGAAAAGGC - 3'; BECN1 forward: 5' - GTGGCTTTCC TGGACTGTGT - 3′ and reverse: 5' - CACTGCCTCCTGTGTCTTCA - 3'; ATG5 forward: 5' - TGCAGATGGACAGTTGCACA - 3′ and reverse: 5' - CCACTGCAGAGGTGTTTCCA - 3'; ATG7 forward: 5' - AGAACATGGTG CTGGTTTCC - 3′ and reverse: 5' – CATCCAGGGTACTGGGCTAA - 3'; ATG12 forward: 5' - AAGTGGGCAGTAGAGCGAAC - 3′ and reverse: 5' - CACGCCTGAGACTTGCAGTA - 3'.

2.5. Western blot analysis

Western blot was performed as previously described [24]. The following antibodies were used in this study: IFNAR1, Stat1, p-Stat1 (Tyr701), cleaved-PARP, cleaved-caspases3, ATG5 and LC3B (Cell Signaling Technology (CST), Danvers, MA, USA). The P62 antibody was purchased from Abcam (Cambridge, MA, USA). A GAPDH antibody purchased from Proteintech (Rocky Hill, NJ, USA) was used as an internal control. Quantification of the proteins was performed using ImageJ software.

2.6. Immunofluorescence assay

HN4, HN30 and Cal27 cells were grown on Lab-Tek chamber slides (Nunc, Rochesta) to 70% confluency. The cells were fixed in 100% methanol for 15 min at −20 °C, permeabilized with 0.3% Triton X-100 in PBS for 10 min and blocked with 1% BSA in PBS for 1 h. The fixed cells were incubated overnight with anti-LC3B primary antibody, washed in PBS and incubated with Alexa Fluor® 568-conjugated anti-rabbit IgG antibody (Molecular Probes, Oregon) for 1 h. The cells were then stained with 0.5 mg/ml of DAPI to visualize nuclei, mounted on glass slides and observed with an LSM510 confocal laser microscope (Carl Zeiss, Oberkochen, Germany).

2.7. Cell transfection

For cell transfection, HNSCC cells were seeded in a 6-well plate and transfected with 100 nM small interfering RNA (siRNA) using Lipofectamine 3000 (Invitrogen, Carlsbad, CA, USA) according to the manufacturer's instructions. Treatments were administered 24 h after transfection. The sequence of the IFNAR1 siRNA is: 5' – CAUUUCGCA AAGCUCAGAUdTdT – 3'. The sequence of the STAT1 siRNA is: 5' – CGGCUGAAUUUCGGCACCUdTdT - 3'. The sequences of the ATG5 siRNA are #1, 5' – GACCAUGCAAUGGUGGCUUdTdT - 3′ and #2, 5' – GTCCATCTAAGGATGCAATdTdT - 3'. The sequence of the scrambled control is: 5' - UUCUCCGAACGUGUCACGUdTdT - 3'.

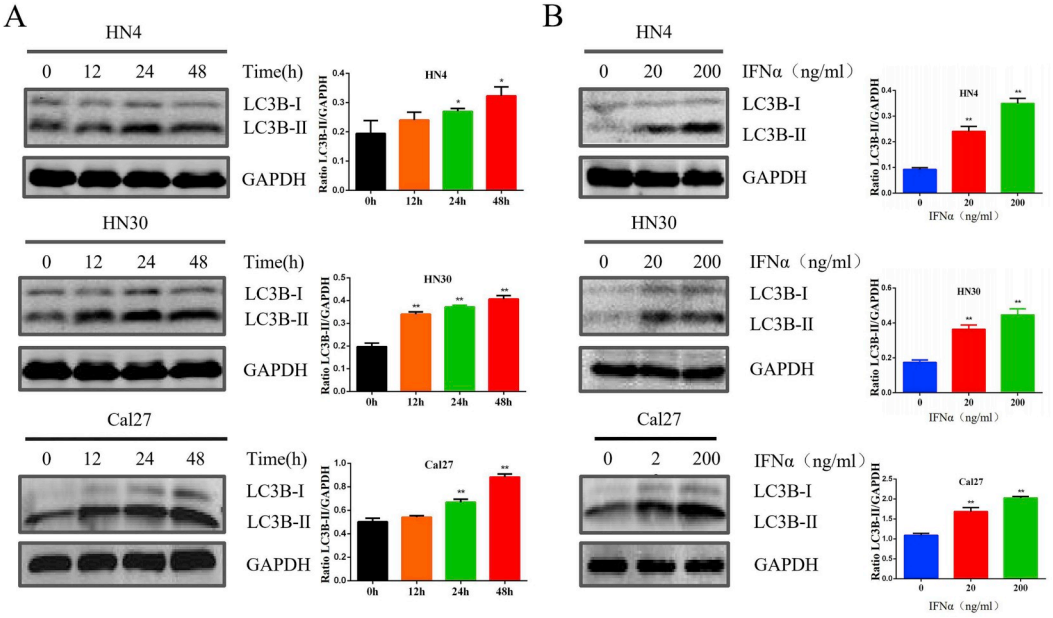

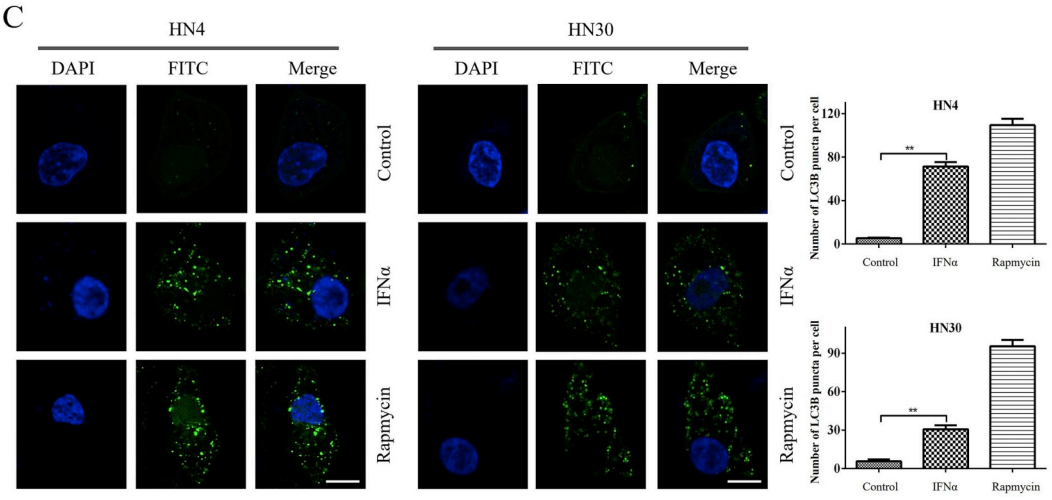

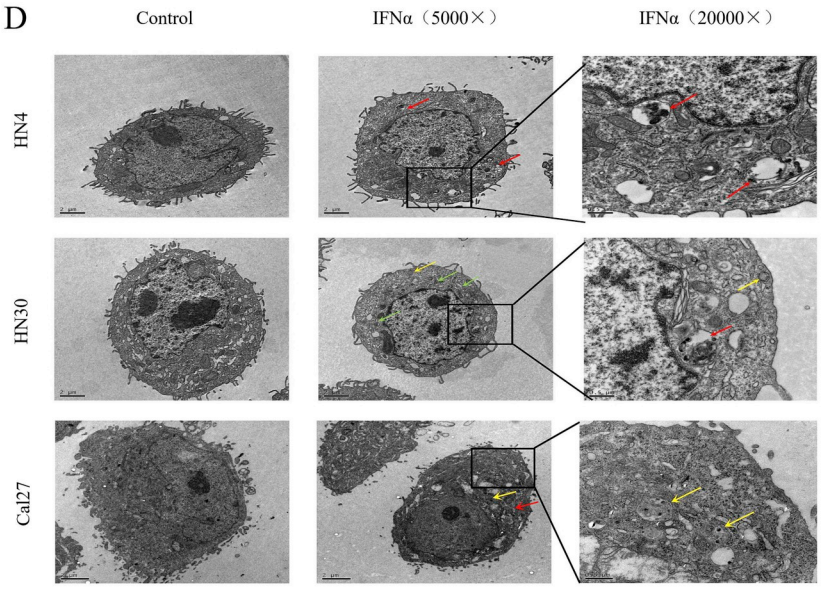

(caption on next page)

Fig. 2. IFNα induces autophagy in HNSCC cells. (A, B) IFNα promoted LC3B-II expression in a concentration- and time-dependent fashion in HNSCC cells. Cells were treated at indicated concentrations of IFNα for multiple time points and LC3B expression was detected by western blotting. Quantification of LC3B-II relative to GAPDH in IFNα-treated HNSCC cells was presented by ImageJ densitometric analysis. (C) IFNα (200 ng/ml) treatment for 24 h increased immunofluorescent LC3B puncta per cell, reflecting an autophagic response in HN4 and HN30 cells. Rapamycin (200 nM) treatment for 24 h was used as a positive control as it is a strong inducer of LC3B puncta. Left, representative immunofluorescent images of HN4 and HN30 cells. Scale bar: 15 μm. Right, quantifications are represented as numbers of LC3B puncta per cell. Statistical values (*t*-test) compare the number of LC3B puncta per cell between conditions. (D) Representative transmission electron microscopy (TEM) images revealing the formation of phagophores (green arrow), autophagosomes (yellow arrow) and autolysosomes (red arrow) after IFNα (200 ng/ml) treatment for 24 h $*P < 0.05$, $**P < 0.01$. (For interpretation of the references to color in this figure legend, the reader is referred to the Web version of this article.)

2.8. Immunohistochemistry

Immunohistochemistry (IHC) was performed as previously described [25]. Briefly, the sections were heated by water bath at 100 °C with EDTA buffer (PH 10.0) for 20 min to retrieve antigen. The primary antibodies were LC3B (CST, Danvers, MA, USA), P62/SQSTM1 (Abcam, Cambridge, MA, UK) and Ki67 (Abcam, Cambridge, MA, UK). Immunohistochemistry and image analysis were performed to measure and analyze the mean optical density for Ki67, P62/SQSTM1 and LC3B in the animal experiments.

2.9. Transmission electron microscopy analysis

HN4, HN30 and Cal27 cells were fixed in 2% paraformaldehyde–glutaraldehyde in 0.1 M phosphate buffer (pH 7.4) and washed in 0.1 M phosphate buffer (PB). Then cells were fixed with 1% OsO4 dissolved in 0.1 M PB for 2 h, dehydrated in an ascending gradual series (50–100%) of ethanol and infiltrated with propylene oxide. Specimens were embedded using the Poly/Bed 812 kit (Polysciences). Then, samples were subjected to pure fresh resin embedding and polymerization at 65 °C in an electron microscope oven (TD-700, DOSAKA, Japan) for 24 h. Sections at about 200–250 nm thick were stained with toluidine blue (Sigma, T3260) and double stained with 6% uranyl acetate (EMS, 20 min) and lead citrate (Fisher, 10 min) for contrast staining. Samples were prepared and analyzed with a JEM 1230 transmission electron microscope (JEOL, USA, Inc.) at 60 kV. Micrographs were obtained at × 5000 and × 20,000 magnifications.

2.10. Drug combination study

As noted in our previous description [17], the combination index (CI) was used to analyze the synergistic inhibitory effects of drug combinations using CompuSyn software. $CI < 1$, $CI = 1$, and $CI > 1$ indicate synergism, an additive effect, and antagonism, respectively.

2.11. Autophagic flux assay

HN4 and HN30 cells were plated in cell culture dishes with glass bottoms. HNSCC cells were transfected with the GFP–mRFP–LC3 construct after cells adhered. Then Human IFNα (PeproTech, Rocky Hill, NJ, USA), wortmannin (Sigma-Aldrich, St Louis, MO, USA) and hydroxychloroquine (Sigma-Aldrich, St Louis, MO, USA) were administered at the indicated concentrations for defined times. The cells were washed twice in ice-cold PBS, fixed, mounted with Histological Mounting Medium (Histomount, USA) and observed using a LSM510 confocal laser microscope (Carl Zeiss, Germany).

2.12. Flow cytometry analysis

HN4 and HN30 cells were treated with IFNα and different autophagy inhibitors for 48 h. Then adherent and floating cells were harvested and detected using the Annexin V–FITC/PI Apoptosis Detection Kit (BD Biosciences, San Diego, CA, USA). Analysis was performed using a BD FORTASA flow cytometer (BD Biosciences) and the FlowJo software.

2.13. In vivo study

SPF BALB/c nude mice (nu/nu, aged 4 weeks, and weighing ~20 g) were purchased from the Shanghai Laboratory Animal Center (Shanghai, China) and were housed in SPF facilities at the Shanghai Ninth People's Hospital, Shanghai Jiao Tong University School of Medicine. The Laboratory Animal Care and Use Committees of the hospital approved all experimental procedures. The nude mouse tumor xenograft model was established with Cal27 cells, an HNSCC cell line exhibiting strong tumorigenicity *in vivo*. In brief, 1×10^6 cells were subcutaneously injected into the right flank of the nude mice. After the xenograft reached a mean diameter of 5 mm, the animals received various treatment regimens: (a) control (0.9% saline, i.p.); (b) IFNα (20, 000 IU per day, s.c.); (c) hydroxychloroquine (60 mg kg^{-1} per day, i.g); (d) wortmannin (0.5 mg kg^{-1} per day, i.p.); (e) IFNα & hydroxychloroquine; and (f) IFNα & wortmannin. Tumor sizes were monitored twice a week. Tumor volumes were calculated using the formula (length × $width^2/2$). Mice were sacrificed and tumor tissues were excised after 4 weeks. Portions of tumor tissues and organs were fixed and embedded in the paraffin. Tissue sections (4 mm) were stained with hematoxylin and eosin. The terminal deoxynucleotidyl transferase dUTP nick end labeling (TUNEL) assay was used to detect apoptotic cells.

2.14. Statistical analysis

Statistical analyses were performed with SPSS 13.0 software for Windows (SPSS Inc., Chicago, IL, USA). Excel and GraphPad Prism version 6 (GraphPad Software, San Diego, CA, USA) were employed to process the initial data and plot the results. The CI was calculated with CompuSyn software to analyze the synergistic inhibitory effects of the drug combinations. Student's *t*-test and one-way analysis of variance were performed to assess the statistical significance of differences. $P < 0.05$ was considered statistically significant. * indicates $P < 0.05$ and ** indicates $P < 0.01$. All values are expressed as the means ± standard deviation.

3. Results

3.1. IFNα exhibits anti-proliferation activity and induces apoptosis in HN4 and HN30 cells

To assess the effects of IFNα on HNSCC cell viability and proliferation, MTT and colony formation assays were performed. IFNα exerted cytotoxicity in a time- and dose-dependent manner in HN4 and HN30 cells (Fig. 1A and B). In addition, IFNα treatment (200 ng/ml) for 10 days potently suppressed the colony forming capacity of HN4 and HN30 cells (Fig. 1C). As shown in Fig. 1D and E, IFNα up-regulated cleaved-PARP and cleaved-caspase3 expressions in a time- and dose-dependent manner in HN4 and HN30 cells. Flow cytometry assays supported the above results, given that the proportion of Annexin V-positive cells increased in a time- and dose-dependent manner after IFNα treatment (Fig. 1F and G). It remained unclear whether IFNα induced autophagy simultaneously with antitumor activity in HNSCC cells.

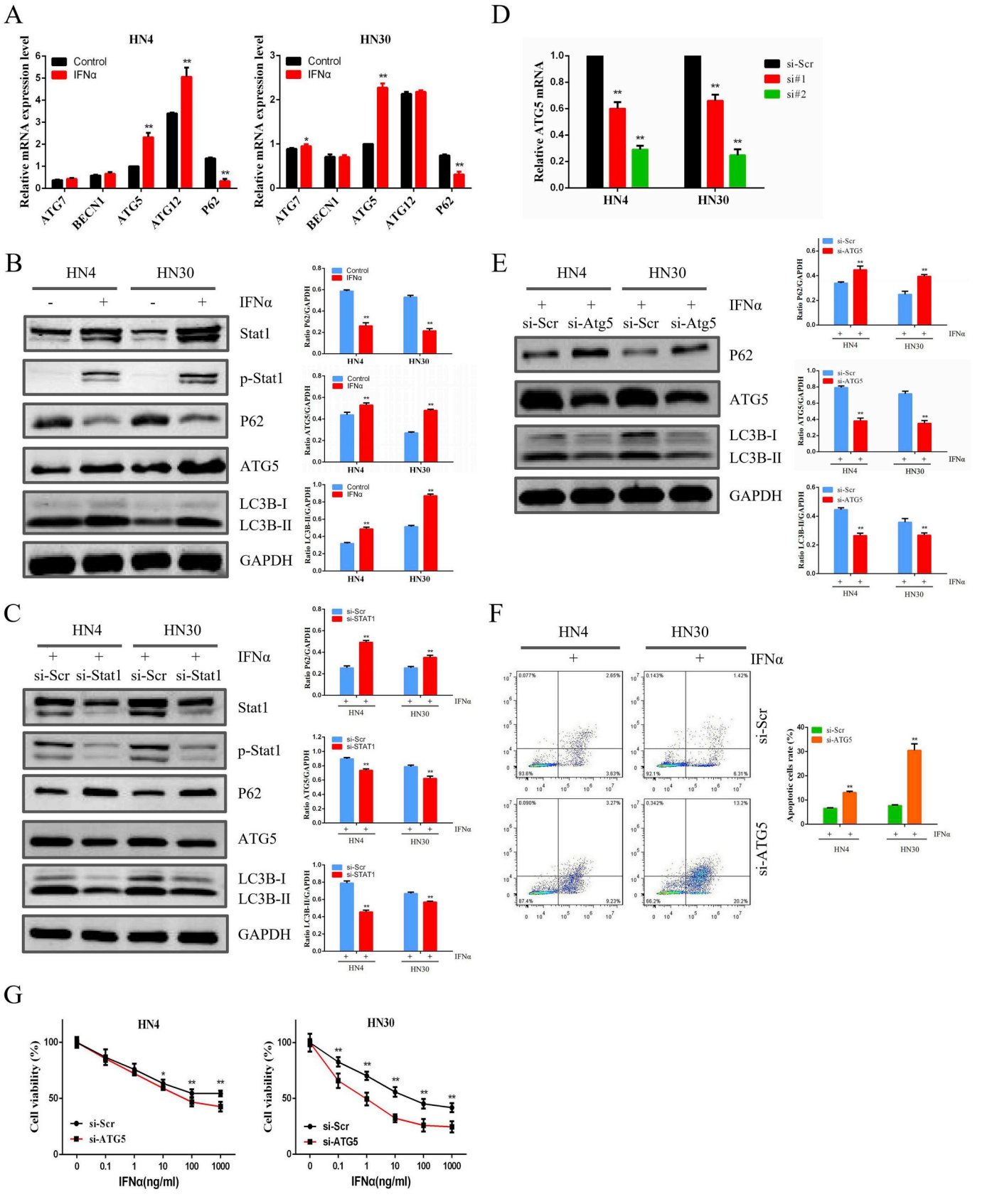

(caption on next page)

Fig. 3. STAT1 and ATG5 are required for IFNα-induced autophagy in HNSCC cells. (A) HN4 and HN30 cells were incubated with IFNα (200 ng/ml) for 48 h, and then the mRNA expressions of these ATGs were analyzed by real-time PCR assay. (B) HN4 and HN30 cells were incubated with IFNα (200 ng/ml) for 48 h. STAT1, p-STAT1, P62, ATG5 and LC3B expressions were detected by western blot. (C) HN4 and HN30 cells were transfected with siRNAs targeting STAT1 for 24 h and then treated with IFNα (200 ng/ml). STAT1, p-STAT1, P62, ATG5 and LC3B expressions were detected by western blotting after 24 h. (D) Efficiency for ATG5 gene silencing was confirmed by real-time PCR assay. (E, F) After transfection with siRNAs against ATG5 for 24 h, HN4 and HN30 cells were treated with IFNα (200 ng/ml). P62, ATG5 and LC3B levels were detected by western blot, and apoptotic cells were measured by flow cytometry analysis of Annexin V and PI staining after 24 h. (G) Twenty-4 h after transfection with siRNAs targeting ATG5, cells were seeded in 96-well plates at a density of 4×10^3 cells per well. Cells were then incubated with the indicated concentrations of IFNα for 72 h. Cell viability was determined by MTT assay. Quantification of P62, ATG5 and LC3B-II relative to GAPDH was presented based on ImageJ densitometric analysis. $^*P < 0.05$, $^{**}P < 0.01$.

3.2. IFNα induces autophagy in HNSCC cells

The amount of LC3B-II conversion is positively related to the formation of autophagosomes during autophagy process. To begin with, we detected LC3B-II expression in four HNSCC cell lines after HCQ treatment. HN4, HN30 and Cal27 showed greater basic autophagy levels (Supplementary Fig. S1). In addition, as shown in Fig. 2A and B, LC3B-II expression increased obviously in IFNα-treated HN4, HN30 and Cal27 cells and represented in a time- and dose-dependent manner, demonstrating autophagy induction by IFNα. Consistently, immunofluorescence assays revealed (Fig. 2C and Supplementary Fig. S2) the increased distribution of LC3B puncta in IFNα-treated HNSCC cells compared with untreated control. Rapamycin was used as a positive control of increased autophagy flux. Furthermore, we examined the morphology of HN4, HN30 and Cal27 cells after exposure to IFNα treatment by transmission electron microscopy (TEM). As shown in Fig. 2D, IFNα activated autophagy flux by increasing the formation of the initial sequestering compartment (the phagophore), autophagosomes often containing multivesicular and multilamellar structures, and autolysosomes. Collectively, our data indicate that IFNα induces autophagy in HNSCC cells.

3.3. STAT1 and ATG5 are required for IFNα-induced autophagy in HN4 and HN30 cells

Autophagy involves a series of dynamic membrane-rearrangement reactions mediated by a core set of autophagy-related genes (ATGs). Among these genes, Beclin1, ATG5, ATG12 and ATG7 represent the major regulators of the classical autophagy pathway in mammalian cells [26]. Using real-time PCR assays (Fig. 3A), we found that IFNα significantly increased the ATG5 mRNA expression in both HN4 and HN30 cells. To ascertain whether the increasing autophagosome formation observed after IFNα treatment was caused by an augmentation of autophagic activity or a reduced turnover of autophagosomes, we analyzed P62/SQSTM1 level. As noted in Fig. 3B, IFNα enhanced P62/SQSTM1 proteolysis and increased the expressions of LC3B-II, ATG5, p-STAT1 and STAT1 simultaneously, indicating that IFNα increased the autophagic flux in HNSCC cells. In addition, IFNAR1 is one of the subunits mediate the signaling of IFNα and induces intracellular signaling cascades. While siRNAs against IFNAR1 decreased IFNAR1 expression (Supplementary Fig. S3), they also significantly inhibited LC3B-II expression in response to IFNα stimulation in HN4 and HN30 cells. Moreover, suppression of STAT1 and ATG5 expression using siRNAs in the context of IFNα treatment (Fig. 3C–E) decreased ATG5 and LC3B-II expressions and increased P62 protein levels. These results suggest that ATG5 and STAT1 are required for IFNα-induced autophagy in HNSCC cells. Moreover, silencing the key regulator of autophagy, ATG5, significantly enhanced the antitumor effects of IFNα using MTT and flow cytometry assays (Fig. 3F and G), indicating that autophagy inhibitors may synergize with IFNα in the treatment of HNSCC.

3.4. Wortmannin and HCQ impair IFNα-induced autophagy in HNSCC cells

Two autophagy inhibitors (wortmannin and HCQ) were applied in our study. We first examined whether wortmannin and HCQ could inhibit autophagy in HNSCC cells. According to previous studies, HCQ treatment results in the accumulation of LC3B-II and P62 proteins. Consistent results were presented in Fig. 4A and B and Supplementary Fig. S4A revealing a time- and dose-dependent response. Wortmannin is an early-stage autophagy inhibitor, which decreased LC3B-II expression and increased P62 expression in a time- and dose-dependent manner in HNSCC cells (Fig. 4C and D and Supplementary Fig. S4B). In addition, western blot analysis (Fig. 4E) demonstrated that wortmannin inhibited autophagy induced by IFNα, and decreased LC3B-II formation and increased P62 protein levels in HN4, HN30 and Cal27 cells. In contrast, the addition of HCQ to IFNα significantly up-regulated LC3B-II and P62 protein levels compared with IFNα treatment alone. Furthermore, autophagy flux assays (Fig. 5) were performed in IFNα-treated HN4 and HN30 cells transfected with a tandem fluorescent-tagged LC3 reporter plasmid (GFP–mRFP–LC3) [27]. The yellow fluorescence of GFP–mRFP–LC3 puncta generated by merging both green and red fluorescence in autophagosomes indicates impaired autophagy, whereas red fluorescence of the mRFP signal alone after fusion with lysosomes implies complete autophagic flux. Our quantification of red (mRFP + GFP-) and yellow (mRFP + GFP+) puncta per cell indicates that IFNα increases autophagy flux (red and yellow puncta). Wortmannin inhibits autophagy flux and HCQ results in the accumulation of yellow puncta (hence autophagosomes) induced by IFNα.

3.5. Autophagy inhibitors synergize with IFNα in antitumor effects in HN4 and HN30 cells

Next, we investigated whether autophagy inhibitors could enhance IFNα-mediated antitumor effects in HNSCC cells. As shown in Fig. 6A, compared with IFNα treatment alone, the combination of IFNα, HCQ and wortmannin significantly increase the proportions of Annexin V-positive HNSCC cells. Moreover, caspase3 and PARP proteins were markedly cleaved in the combined drug groups (Fig. 6B and C). Similarly, the combination of IFNα with wortmannin or HCQ also greatly reduced cell viability in both HN4 and HN30 cells (Fig. 6D). The combination index was calculated using the Chou-Talalay method to further explore the potential synergistic effects of IFNα and autophagy inhibitors in HNSCC cells. As shown in Fig. 6E, all CI values at Fa = 0.5 were below the CI = 1 horizontal dotted line. The numerical values of CI were presented in Table 1 to confirm the synergistic effects of IFNα, wortmannin, and HCQ in HNSCC cells. An IC50(r) ≥ 0.95 suggests a good fit of the curve. Thus, the IFNα, wortmannin, and HCQ combination treatment exerts synergistic effects on HNSCC.

3.6. Autophagy inhibitors enhance the antitumor effects of IFNα treatment in vivo

Finally, we confirmed the *in vitro* results using human HNSCC xenografts in nude mice. First, the tumor volumes significantly ($P < 0.01$) reduced in the combined drug group compared with groups treated with each individual agent (Fig. 7A and B). According to TUNEL assay results (Fig. 7C), IFNα increased the number of apoptotic cells *in vivo* when mice were treated with wortmannin or HCQ together. We did not observe significant toxic effects on important organs in any treatment group (Supplementary Fig. S5). In addition, H&E staining of HNSCC xenografts revealed fibrous connective tissue with unusual

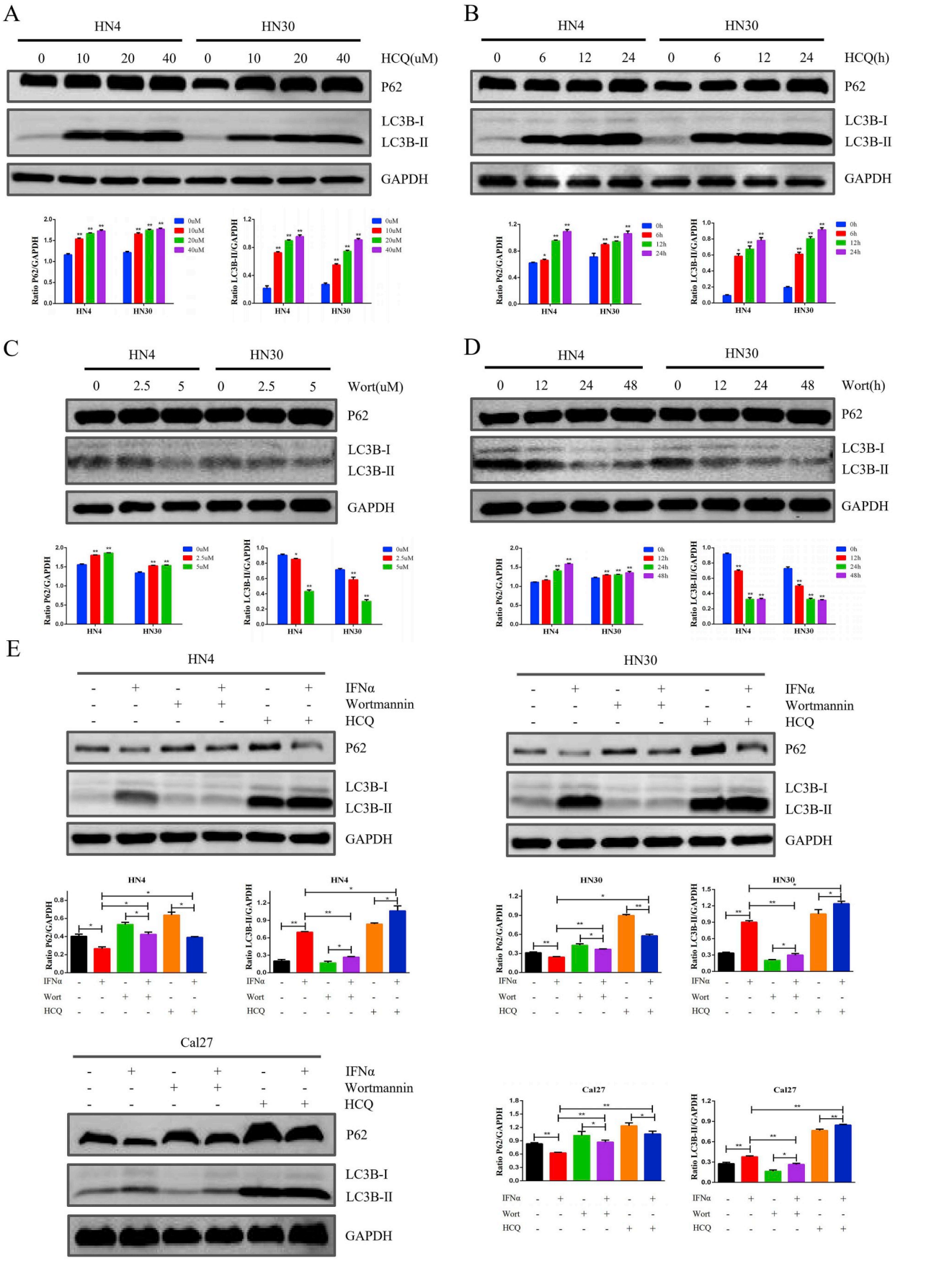

(caption on next page)

Fig. 4. Wortmannin and HCQ impair IFNα-induced autophagy in HNSCC cells. (A) Western blot of P62 and LC3B expression in HN4 and HN30 cells after 0, 10, 20, and 40 μM HCQ treatment for 24 h. (B) P62 and LC3B expressions were detected by western blot in HN4 and HN30 cells treated with 10 μM HCQ at the indicated times. (C) Western blot of p62 and LC3B expression in HN4 and HN30 cells after 0, 2.5 and 5 μM wortmannin treatment for 48 h. (D) P62 and LC3B expressions were detected by western blot in HN4 and HN30 cells under 5 μM wortmannin treatment at indicated times. (E) HN4, HN30 and Cal27 cells were incubated with or without 200 ng/ml of IFNα for 48 h in the presence or absence of the autophagy inhibitors wortmannin (5 μM) for 48 h or HCQ (10 μM) for 12 h. P62 and LC3B expressions were detected in HN4 and HN30 cells by western blot. Quantification of P62 and LC3B-II relative to GAPDH was presented based on ImageJ densitometric analysis. $*P < 0.05$, $**P < 0.01$.

amounts of extracellular matrix rich in fibroblasts and vascular vessels (Fig. 7D). Furthermore, immunohistochemistry (Fig. 7D) of tumor tissues revealed reduced Ki67 expression, a marker of proliferation, in the combined drug groups compared with the individual drug group. In accordance with *in vitro* results, wortmannin decreased LC3B-II expression and increased P62 protein levels when combined with IFNα or used alone, whereas HCQ resulted in accumulation of both LC3B-II and P62 proteins. In summary, IFNα can induce autophagy and exhibit synergistic effects with wortmannin or HCQ on suppressing tumor growth *in vivo* (Fig. 7E).

4. Discussion

In our study, we demonstrate that IFNα induces autophagy, and blockade of autophagy also enhances the killing effect mediated by IFNα in HNSCC. IFNα-induced autophagy may partly explain the

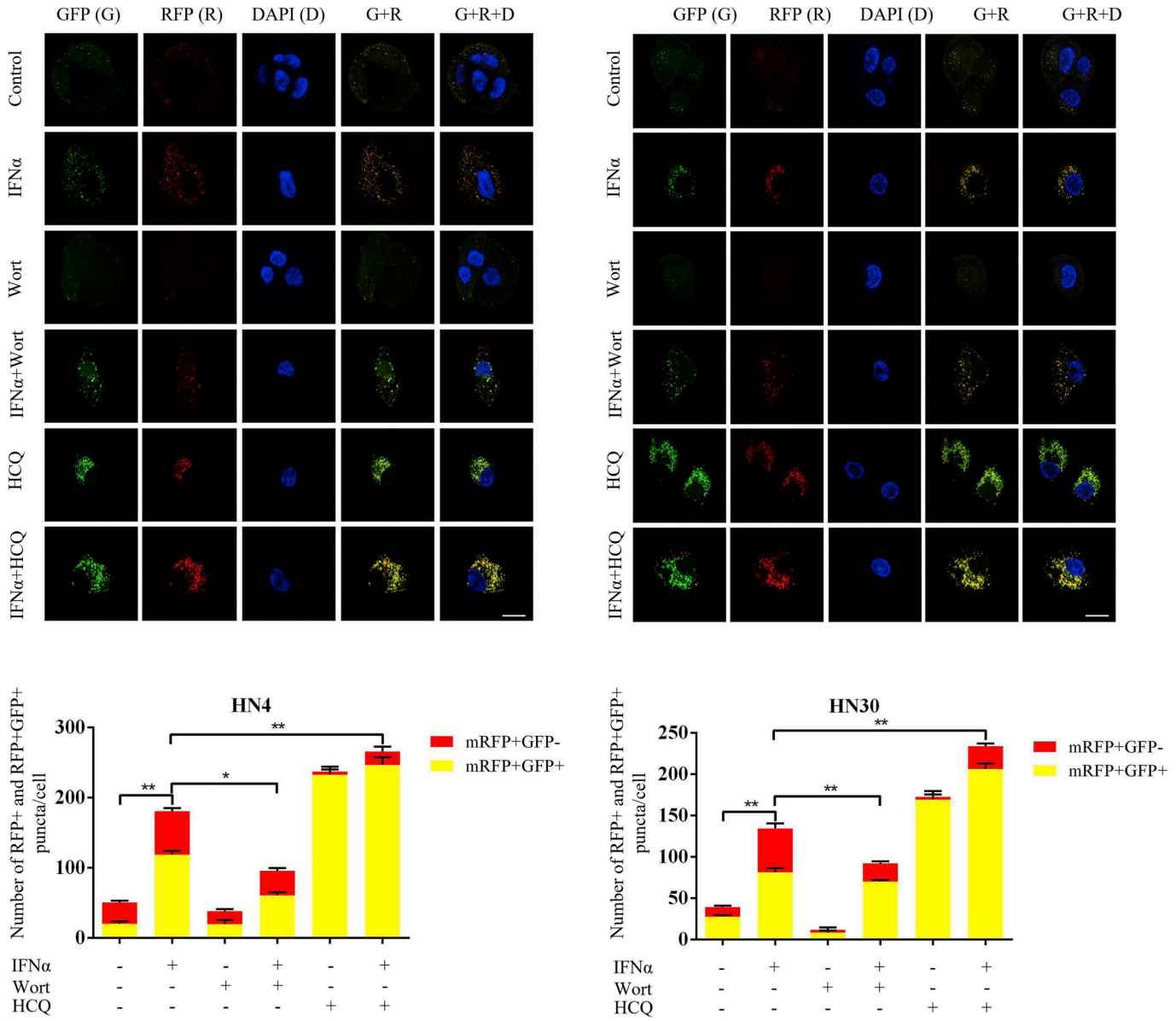

Fig. 5. Application of GFP–mRFP–LC3 plasmid to examine autophagy flux in HNSCC cells. HN4 and HN30 cells were transfected with GFP–mRFP–LC3 construct and then exposed to IFNα (200 ng/ml) for 48 h combined with wortmannin for 48 h or HCQ for 12 h. Then the merged color was observed in treated HNSCC cells using a confocal laser microscope. Scale bar: 25 μm. Quantitative analysis of red and yellow LC3 puncta was reported as mean ± SD. $*P < 0.05$, $**P < 0.01$. (For interpretation of the references to color in this figure legend, the reader is referred to the Web version of this article.)

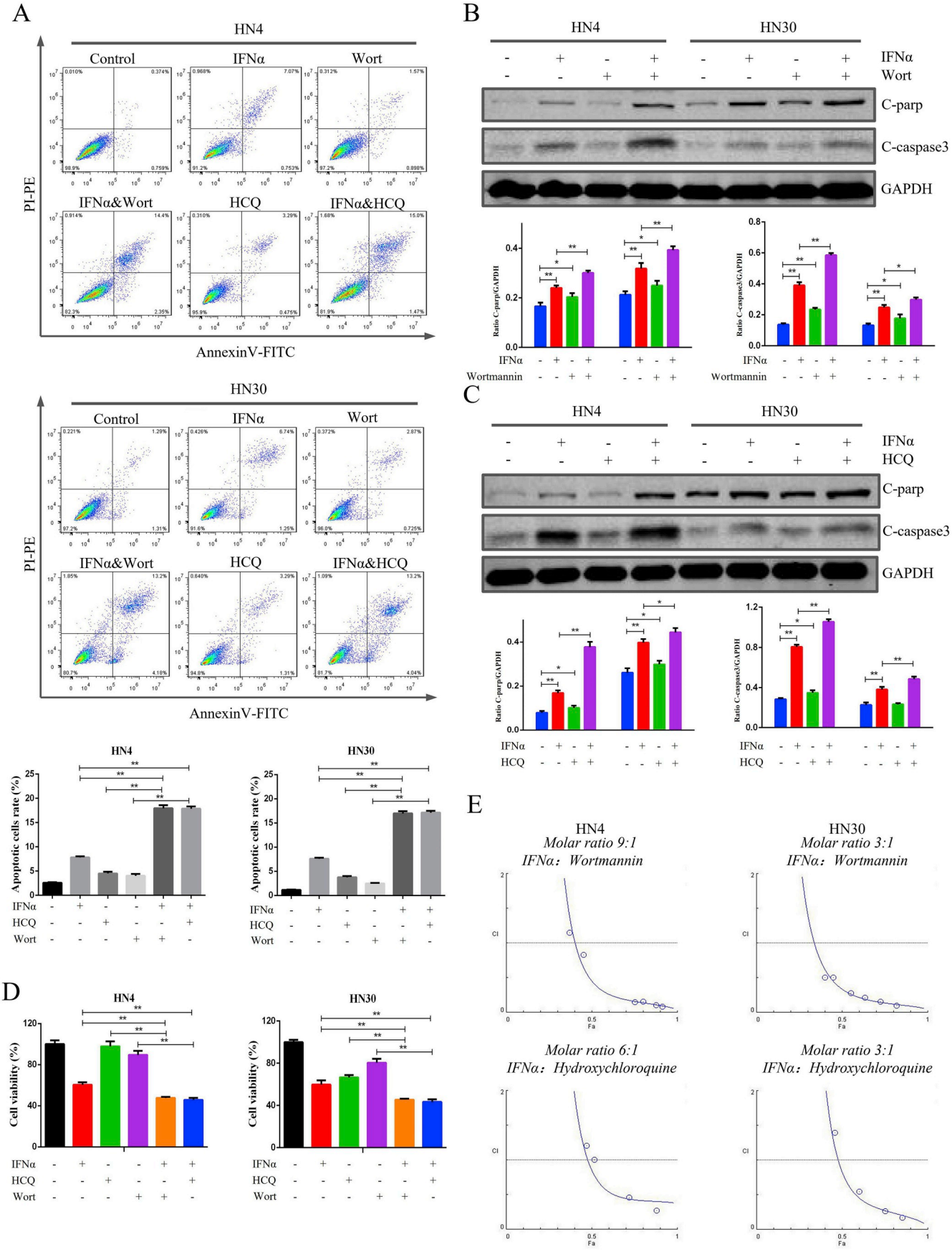

(caption on next page)

Fig. 6. Autophagy inhibitors enhance growth inhibition and promote apoptosis induced by IFNα in HNSCC cells. (A) IFNα increased the fraction of apoptotic HN4 and HN30 cells after treatment with autophagy inhibitors wortmannin and HCQ for 48 h as measured by flow cytometry analysis of Annexin V and PI staining. (B, C) HN4 or HN30 cells were incubated with or without 100 ng/ml of IFNα in the presence or absence of the autophagy inhibitors wortmannin (5 μM) or HCQ (10 μM) for 48 h. Whole protein was extracted, and cleaved-caspase3 and cleaved-PARP were analyzed by western blot. Quantification of cleaved-PARP and cleaved-caspase3 relative to GAPDH was presented based on ImageJ densitometric analysis. (D) Cell growth inhibition was analyzed by MTT. (E) Effects of treatments with combination of IFNα and wortmannin or HCQ on HN4 and HN30 cell lines. The CI/fractional effect curve (Fa) revealed the CI versus the fraction of cells affected/inhibited by the combination treatment in different cell lines. For each cell line, the molar ratio of equipotent doses of the two agents (at the ratio of their $IC50_S$) is presented. Combination analysis was performed using CompuSyn software. $^*P < 0.05$, $^{**}P < 0.01$.

unsatisfactory effect of IFNα in solid tumors. Moreover, we observe clear synergistic antitumor effects of IFNα, wortmannin, and HCQ in the median drug analysis and CI calculation. This finding is of great significance to the clinical application of the combination treatment with IFNα and autophagy inhibitors in HNSCC.

IFNα is a double-edged sword in cancers, as it not only performs antiviral, anti-proliferative and immunomodulatory functions but also has a negative role by promoting negative feedback and immunosuppression [28–30]. Cumulative evidences also suggest that IFNα treatment is most beneficial against early or disseminated cancer, but much less effective against established and metastatic tumors. This phenomenon seems to have something in common with autophagy, which plays a dual role in tumor progression. Consistent with our hypothesis, a previous study demonstrates that IFNα induces autophagy in certain human cancer cell lines, such as human Burkitt lymphoma Daudi cells and human glioblastoma T98G cells [31]. However, no study has been performed to examine this phenomenon in animal models. In our study, *in vitro* and *in vivo* experimental procedures were undertaken to verify the presence of autophagy in HNSCC after IFNα treatment. Because IFNα has not yet been approved for most solid tumors including HNSCC, the autophagy activation in HNSCC tissues cannot be detected. Unfortunately, there is also no literature on autophagy activation in cancers with IFNα therapy. Furthermore, there is no sufficient evidence that interferon signaling pathway shows positive association with autophagy markers in HNSCC tissues. Collectively, our study is the first to demonstrate that IFNα induces autophagy in HNSCC, providing a strong evidence to explain the low response rate of IFNα therapy in solid tumors.

Autophagy is highly dependent on the availability of the so-called autophagy-related proteins (ATGs) [32]. Our results show that genetic inhibition of autophagy through silencing ATG5 promotes IFNα-mediated growth inhibition and apoptosis, demonstrating the cytoprotective role of autophagy during IFNα treatment. Indeed, existing reports suggest that knockdown of the essential autophagy component ATG5 enhances chemosensitivity to efficiently eliminate cancer cells [33,34]. Inhibition of autophagy by blocking ATG5 may contribute to treatment for advanced tumors.

Although the process of autophagy is complex and how it should be manipulated when treating patients is not fully defined [35], several pharmacologic mediators of autophagy are used in clinical trials. Indeed, our results demonstrate that pharmacologic inhibition of autophagy with wortmannin and HCQ increases the antitumor activity of IFNα, which provides a strong rationale for assessing the therapeutic efficacy of IFNα in combination with autophagy inhibitors (HCQ and wortmannin) as a treatment for HNSCC in future clinical trials. The lysosomotropic agent HCQ can inhibit autophagy to some extent and has been used in several preclinical and clinical trials for sensitizing tumors to chemotherapy [36–39]. In our study, HCQ is chosen as an autophagy inhibitor instead of CQ, because it is less toxic than CQ at peak concentrations [40,41]. In addition, our results demonstrate that HCQ sensitizes HNSCC to IFNα through enhancing apoptosis *in vitro* and *in vivo*. Wortmannin is a potent inhibitor of phosphoinositide 3-kinases (PI3-Ks) and one of the most commonly used autophagy inhibitors. Studies have also demonstrated that wortmannin is both a chemosensitizer [42] and a radiosensitizer [43]. However, at higher doses, less specific and potent agents such as 3-MA will inhibit class I PI3K, thereby paradoxically activating autophagy [44]. A recent study in HNSCC also observed that 25 μM 3-MA downregulated mTOR signaling. Unlike HCQ, 3-MA did not have a notable effect on CYT997-induced apoptotic death and repression of cell survival [45]. In contrast, our results show that wortmannin suppresses autophagy *in vitro* and *in vivo*, and combination of wortmannin and IFNα significantly inhibits HNSCC tumor growth.

In summary, we have demonstrated that IFNα significantly induces autophagy in HNSCC cells and inhibition of autophagy by the autophagy inhibitors wortmannin and HCQ can enhance the antitumor effects of IFNα in HNSCC cells. This study provides a new strategy to enhance the efficacy of IFNα in cancer treatment and may encourage the development of an autophagy inhibitor to improve IFNα treatment for HNSCC.

Conflicts of interest

The authors declare no conflict of interest.

Author contributions

H. Ma, M. Ruan, J. Hu: conception and design. W. Yang, C. Jiang, H. Ju, S. Jin, S. Liu, L. Zhang: acquisition and interpretation of data. W. Yang, C. Jiang: drafting of the manuscript. W. Yang, C. Jiang, G. Ren, W. Xia: statistical analysis. H. Ma, M. Ruan, J. Hu: obtained funding.

Table 1
IC50 (r), IC50, and CI for IFNα combination treatment.

Cell lines	IC50(r)	IC50			CI
		IFNα(ng/ml)	Wortmannin(μm)	Hydroxychloroquine(μm)	
HN4	0.98382	480.37000	52.57300	–	0.449480
	0.95099		–	84.09550	0.848450
HN30	0.99345	202.87800	60.52760	–	0.335790
	0.97490		–	69.63510	0.82480

Abbreviations: CI = combination index; IFNα = interferon-alpha; IC50 (r) represents the correlation coefficient for the fit between the CI and Fa; CIs were calculated for ED50 using an isobologram analysis generated with CompuSyn software.

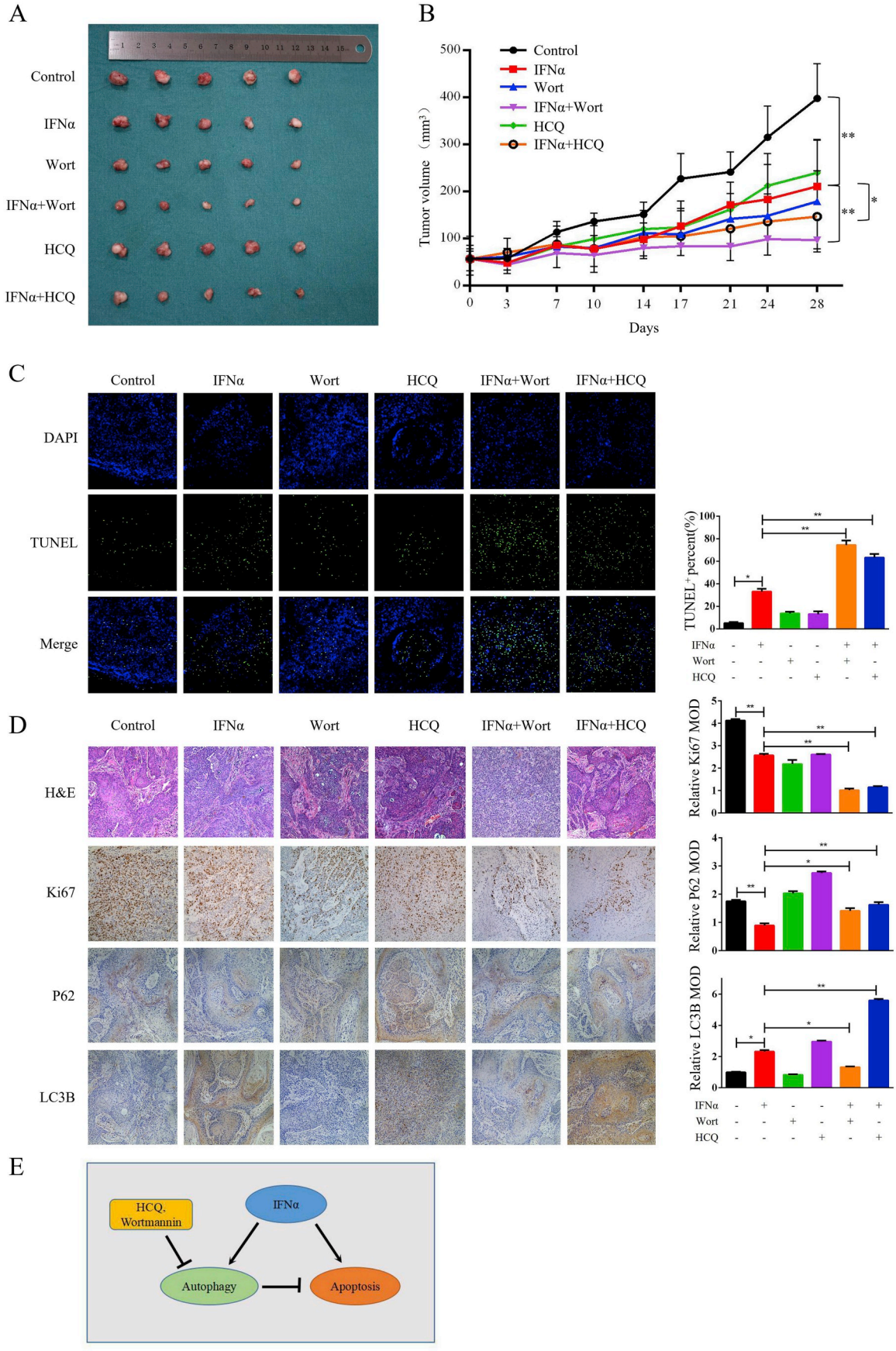

(caption on next page)

Fig. 7. Autophagy inhibitors enhance antitumor effects of IFNα therapy *in vivo*. After establishing the HNSCC tumor xenograft model, 30 nude mice were randomly divided into six groups (five mice per group). The groups received the following treatments: IFNα (20, 000 IU per mouse per day, s.c.), wortmannin (0.5 mg/kg per day, i.p), HCQ (60 mg/kg per day, i.g), IFNα plus wortmannin, IFNα plus HCQ, and control (0.9% saline, i.p). All mice were sacrificed 28 days after treatment. (A) Representative images of subcutaneous tumors after treatment. (B) The tumor volumes were analyzed and compared among the groups. Data were expressed as the mean ± SD. (C) The percentage of TUNEL-positive cells was assessed in formalin-fixed paraffin embedding sections of tumors from each group. Magnification: × 200. (D) Representative images of tumor H&E staining from xenograft mouse models and representative images of IHC of Ki67, P62 and LC3B expression from xenograft mouse models. (E) Schematic diagram showing that blocking autophagy by wortmannin and hydroxychloroquine promoted IFNα-mediated apoptosis. Magnification: × 200. $^{*}P < 0.05$, $^{**}P < 0.01$.

Acknowledgments

This study was supported by the National Natural Science Foundation of China (grant numbers 81472516, 81872185, 31140007, 81772870 and 81472517); the Natural Science Foundation of Shanghai (grant number 14ZR1424200); the Shanghai Leading Academic Discipline Project (grant number S30206); and the Doctoral Innovation Fund of Shanghai Jiao Tong University School of Medicine (grant number BXJ201728).

Appendix A. Supplementary data

Supplementary data to this article can be found online at https://doi.org/10.1016/j.canlet.2019.02.052.

References

[1] R.L. Siegel, K.D. Miller, A. Jemal, Cancer statistics, 2019, CA - Cancer J. Clin. 69 (2019) 7–34.
[2] S. Baxi, M. Fury, I. Ganly, S. Rao, D.G. Pfister, Ten years of progress in head and neck cancers, J. Natl. Compr. Cancer Netw. 10 (2012) 806–810.
[3] R. Amaravadi, A.C. Kimmelman, E. White, Recent insights into the function of autophagy in cancer, Genes Dev. 30 (2016) 1913–1930.
[4] A.C. Kimmelman, E. White, Autophagy and tumor metabolism, Cell Metabol. 25 (2017) 1037–1043.
[5] J.S. Muhammad, S. Nanjo, T. Ando, S. Yamashita, T. Maekita, T. Ushijima, Y. Tabuchi, T. Sugiyama, Autophagy impairment by Helicobacter pylori-induced methylation silencing of MAP1LC3Av1 promotes gastric carcinogenesis, Int. J. Cancer 140 (2017) 2272–2283.
[6] S. Shen, M. Zhou, K. Huang, Y. Wu, Y. Ma, J. Wang, J. Ma, S. Fan, Blocking autophagy enhances the apoptotic effect of 18beta-glycyrrhetinic acid on human sarcoma cells via endoplasmic reticulum stress and JNK activation, Cell Death Dis. 8 (2017) e3055.
[7] P. Kong, X. Zhu, Q. Geng, L. Xia, X. Sun, Y. Chen, W. Li, Z. Zhou, Y. Zhan, D. Xu, The microRNA-423-3p-bim Axis promotes cancer progression and activates oncogenic autophagy in gastric cancer, Mol. Ther. 25 (2017) 1027–1037.
[8] J. Wang, Z. Liu, T. Hu, L. Han, S. Yu, Y. Yao, Z. Ruan, T. Tian, T. Huang, M. Wang, L. Jing, K. Nan, X. Liang, Nrf2 promotes progression of non-small cell lung cancer through activating autophagy, Cell Cycle 16 (2017) 1053–1062.
[9] Y. Lei, B.A. Kansy, J. Li, L. Cong, Y. Liu, S. Trivedi, H. Wen, J.P. Ting, H. Ouyang, R.L. Ferris, EGFR-targeted mAb therapy modulates autophagy in head and neck squamous cell carcinoma through NLRX1-TUFM protein complex, Oncogene 35 (2016) 4698–4707.
[10] I. Chang, C.Y. Wang, Inhibition of HDAC6 protein enhances bortezomib-induced apoptosis in head and neck squamous cell carcinoma (HNSCC) by reducing autophagy, J. Biol. Chem. 291 (2016) 18199–18209.
[11] L. Zhang, W. Zhang, Y.F. Wang, B. Liu, W.F. Zhang, Y.F. Zhao, A.B. Kulkarni, Z.J. Sun, Dual induction of apoptotic and autophagic cell death by targeting survivin in head neck squamous cell carcinoma, Cell Death Dis. 6 (2015) e1771.
[12] K.C. Li, K.T. Hua, Y.S. Lin, C.Y. Su, J.Y. Ko, M. Hsiao, M.L. Kuo, C.T. Tan, Inhibition of G9a induces DUSP4-dependent autophagic cell death in head and neck squamous cell carcinoma, Mol. Cancer 13 (2014) 172.
[13] B.S. Parker, J. Rautela, P.J. Hertzog, Antitumour actions of interferons: implications for cancer therapy, Nat. Rev. Cancer 16 (2016) 131–144.
[14] K.K. Mukherjee, A. Bose, D. Ghosh, K. Sarkar, S. Goswami, S. Pal, J. Biswas, R. Baral, IFNalpha2b augments immune responses of cisplatin + 5-fluorouracil treated tongue squamous cell carcinoma patients–a preliminary study, Indian J. Med. Res. 136 (2012) 54–59.
[15] X. Zhang, Z.G. Chen, F.R. Khuri, D.M. Shin, Induction of cell cycle arrest and apoptosis by a combined treatment with 13-cis-retinoic acid, interferon-alpha2a, and alpha-tocopherol in squamous cell carcinoma of the head and neck, Head Neck 29 (2007) 351–361.
[16] X. Liu, J. Lu, M.L. He, Z. Li, B. Zhang, L.H. Zhou, Q. Li, G. Li, L. Wang, W.D. Tian, Y. Peng, X.P. Li, Antitumor effects of interferon-alpha on cell growth and metastasis in human nasopharyngeal carcinoma, Curr. Cancer Drug Targets 12 (2012) 561–570.
[17] H. Ma, S. Jin, W. Yang, G. Zhou, M. Zhao, S. Fang, Z. Zhang, J. Hu, Interferon-alpha enhances the antitumour activity of EGFR-targeted therapies by upregulating RIG-I in head and neck squamous cell carcinoma, Br. J. Cancer 118 (2018) 509–521.
[18] H.B. Muss, R.A. Kempf, S. Martino, S.A. Rudnick, J. Greiner, M.R. Cooper, D. Decker, S.M. Grunberg, D.V. Jackson, F. Richards 2ndet al., A phase II study of recombinant alpha interferon in patients with recurrent or metastatic breast cancer, J. Clin. Oncol. 2 (1984) 1012–1016.
[19] G.D. Hall, J.M. Brown, R.E. Coleman, M. Stead, K.S. Metcalf, K.R. Peel, C. Poole, M. Crawford, B. Hancock, P.J. Selby, T.J. Perren, Maintenance treatment with interferon for advanced ovarian cancer: results of the Northern and Yorkshire gynaecology group randomised phase III study, Br. J. Cancer 91 (2004) 621–626.
[20] A. Pagotto, G. Pilotto, E.L. Mazzoldi, M.O. Nicoletto, S. Frezzini, A. Pasto, A. Amadori, Autophagy inhibition reduces chemoresistance and tumorigenic potential of human ovarian cancer stem cells, Cell Death Dis. 8 (2017) e2943.
[21] G. Pei, M. Luo, X. Ni, J. Wu, S. Wang, Y. Ma, J. Yu, Autophagy facilitates metadherin-induced chemotherapy resistance through the AMPK/ATG5 pathway in gastric cancer, Cell. Physiol. Biochem. 46 (2018) 847–859.
[22] J.M. Mulcahy Levy, S. Zahedi, A.M. Griesinger, A. Morin, K.D. Davies, D.L. Aisner, B.K. Kleinschmidt-Demasters, B.E. Fitzwalter, M.L. Goodall, J. Thorburn, V. Amani, A.M. Donson, D.K. Birks, D.M. Mirsky, T.C. Hankinson, M.H. Handler, A.L. Green, R. Vibhakar, N.K. Foreman, A. Thorburn, Autophagy inhibition overcomes multiple mechanisms of resistance to BRAF inhibition in brain tumors, Elife 6 (2017) e19671.
[23] S. Jin, H. Ma, W. Yang, H. Ju, L. Wang, Z. Zhang, Cell division cycle 7 is a potential therapeutic target in oral squamous cell carcinoma and is regulated by E2F1, J. Mol. Med. 96 (2018) 513–525.
[24] S.F. Jin, H.L. Ma, Z.L. Liu, S.T. Fu, C.P. Zhang, Y. He, XL413, a cell division cycle 7 kinase inhibitor enhanced the anti-fibrotic effect of pirfenidone on TGF-beta1-stimulated C3H10T1/2 cells via Smad2/4, Exp. Cell Res. 339 (2015) 289–299.
[25] H.L. Ma, S.F. Jin, W.T. Ju, Y. Fu, Y.Y. Tu, L.Z. Wang, L. Jiang, Z.Y. Zhang, L.P. Zhong, Stathmin is overexpressed and regulated by mutant p53 in oral squamous cell carcinoma, J. Exp. Clin. Cancer Res. 36 (2017) 109.
[26] C. Burman, N.T. Ktistakis, Autophagosome formation in mammalian cells, Semin. Immunopathol 32 (2010) 397–413.
[27] S. Kimura, T. Noda, T. Yoshimori, Dissection of the autophagosome maturation process by a novel reporter protein, tandem fluorescent-tagged LC3, Autophagy 3 (2007) 452–460.
[28] S. Terawaki, S. Chikuma, S. Shibayama, T. Hayashi, T. Yoshida, T. Okazaki, T. Honjo, IFN-alpha directly promotes programmed cell death-1 transcription and limits the duration of T cell-mediated immunity, J. Immunol. 186 (2011) 2772–2779.
[29] J.L. Benci, B. Xu, Y. Qiu, T.J. Wu, H. Dada, C. Twyman-Saint Victor, L. Cucolo, D.S.M. Lee, K.E. Pauken, A.C. Huang, T.C. Gangadhar, R.K. Amaravadi, L.M. Schuchter, M.D. Feldman, H. Ishwaran, R.H. Vonderheide, A. Maity, E.J. Wherry, A.J. Minn, Tumor interferon signaling regulates a multigenic resistance program to immune checkpoint blockade, Cell 167 (2016) 1540–1554.
[30] H. Ma, W. Yang, L. Zhang, S. Liu, M. Zhao, G. Zhou, L. Wang, S. Jin, Z. Zhang, J. Hu, Interferon-alpha promotes immunosuppression through IFNAR1/STAT1 signalling in head and neck squamous cell carcinoma, Br. J. Cancer 120 (2019) 317–330.
[31] H. Schmeisser, S.B. Fey, J. Horowitz, E.R. Fischer, C.A. Balinsky, K. Miyake, J. Bekisz, A.L. Snow, K.C. Zoon, Type I interferons induce autophagy in certain human cancer cell lines, Autophagy 9 (2013) 683–696.
[32] C.F. Bento, M. Renna, G. Ghislat, C. Puri, A. Ashkenazi, M. Vicinanza, F.M. Menzies, D.C. Rubinsztein, Mammalian autophagy: how does it work? Annu. Rev. Biochem. 85 (2016) 685–713.
[33] Y. Zheng, C. Su, L. Zhao, Y. Shi, Chitosan nanoparticle-mediated co-delivery of shAtg-5 and gefitinib synergistically promoted the efficacy of chemotherapeutics through the modulation of autophagy, J. Nanobiotechnol. 15 (2017) 28.
[34] J. Zhong, X. Dong, P. Xiu, F. Wang, J. Liu, H. Wei, Z. Xu, F. Liu, T. Li, J. Li, Blocking autophagy enhances meloxicam lethality to hepatocellular carcinoma by promotion of endoplasmic reticulum stress, Cell Prolif 48 (2015) 691–704.
[35] C.G. Towers, A. Thorburn, Therapeutic targeting of autophagy, Ebiomedicine 14 (2016) 15–23.
[36] D.T. Vogl, E.A. Stadtmauer, K.S. Tan, D.F. Heitjan, L.E. Davis, L. Pontiggia, R. Rangwala, S. Piao, Y.C. Chang, E.C. Scott, T.M. Paul, C.W. Nichols, D.L. Porter, J. Kaplan, G. Mallon, J.E. Bradner, R.K. Amaravadi, Combined autophagy and proteasome inhibition: a phase 1 trial of hydroxychloroquine and bortezomib in patients with relapsed/refractory myeloma, Autophagy 10 (2014) 1380–1390.
[37] D. Mahalingam, M. Mita, J. Sarantopoulos, L. Wood, R.K. Amaravadi, L.E. Davis, A.C. Mita, T.J. Curiel, C.M. Espitia, S.T. Nawrocki, F.J. Giles, J.S. Carew, Combined autophagy and HDAC inhibition: a phase I safety, tolerability, pharmacokinetic, and pharmacodynamic analysis of hydroxychloroquine in combination with the HDAC inhibitor vorinostat in patients with advanced solid tumors, Autophagy 10 (2014) 1403–1414.
[38] R. Rangwala, Y.C. Chang, J. Hu, K.M. Algazy, T.L. Evans, L.A. Fecher, L.M. Schuchter, D.A. Torigian, J.T. Panosian, A.B. Troxel, K.S. Tan, D.F. Heitjan, A.M. Demichele, D.J. Vaughn, M. Redlinger, A. Alavi, J. Kaiser, L. Pontiggia,

L.E. Davis, P.J. O'dwyer, R.K. Amaravadi, Combined MTOR and autophagy inhibition: phase I trial of hydroxychloroquine and temsirolimus in patients with advanced solid tumors and melanoma, Autophagy 10 (2014) 1391–1402.
[39] K.L. Cook, A. Warri, D.R. Soto-Pantoja, P.A. Clarke, M.I. Cruz, A. Zwart, R. Clarke, Hydroxychloroquine inhibits autophagy to potentiate antiestrogen responsiveness in ER+ breast cancer, Clin. Cancer Res. 20 (2014) 3222–3232.
[40] R.A. Barnard, L.A. Wittenburg, R.K. Amaravadi, D.L. Gustafson, A. Thorburn, D.H. Thamm, Phase I clinical trial and pharmacodynamic evaluation of combination hydroxychloroquine and doxorubicin treatment in pet dogs treated for spontaneously occurring lymphoma, Autophagy 10 (2014) 1415–1425.
[41] D.C. Warhurst, J.C. Steele, I.S. Adagu, J.C. Craig, C. Cullander, Hydroxychloroquine is much less active than chloroquine against chloroquine-resistant Plasmodium falciparum, in agreement with its physicochemical properties, J. Antimicrob. Chemother. 52 (2003) 188–193.
[42] J.M. Caster, M. Sethi, S. Kowalczyk, E. Wang, X. Tian, S. Nabeel Hyder, K.T. Wagner, Y.A. Zhang, C. Kapadia, K. Man Au, A.Z. Wang, Nanoparticle delivery of chemosensitizers improve chemotherapy efficacy without incurring additional toxicity, Nanoscale 7 (2015) 2805–2811.
[43] S. Karve, M.E. Werner, R. Sukumar, N.D. Cummings, J.A. Copp, E.C. Wang, C. Li, M. Sethi, R.C. Chen, M.E. Pacold, A.Z. Wang, Revival of the abandoned therapeutic wortmannin by nanoparticle drug delivery, Proc. Natl. Acad. Sci. U.S.A. 109 (2012) 8230–8235.
[44] Y.T. Wu, H.L. Tan, G. Shui, C. Bauvy, Q. Huang, M.R. Wenk, C.N. Ong, P. Codogno, H.M. Shen, Dual role of 3-methyladenine in modulation of autophagy via different temporal patterns of inhibition on class I and III phosphoinositide 3-kinase, J. Biol. Chem. 285 (2010) 10850–10861.
[45] L. Gao, X. Zhao, L. Lang, C. Shay, W. Andrew Yeudall, Y. Teng, Autophagy blockade sensitizes human head and neck squamous cell carcinoma towards CYT997 through enhancing excessively high reactive oxygen species-induced apoptosis, J. Mol. Med. 96 (2018) 929–938.